Electronic Supplementary Material (ESI) for Journal of Materials Chemistry A.

The salt-resistant solar evaporator with organic diradicaloids as photothermal materials for efficient and persistent desalination

Shuo Qi,[a] Liuzhong Yuan,[b] Shuqing Ao,[a] Luoqing Wang,[a] Tao Jia*[a] and Chuandong Dou*[b]

a. Key Laboratory of Forest Plant Ecology, Ministry of Education, Engineering Research Center of Forest Bio-Preparation, College of Chemistry, Chemical Engineering and Resource Utilization, Northeast Forestry University, Harbin 150040, China, E-mail: jiataopolychem@nefu.edu.cn

b. State Key Laboratory of Supramolecular Structure and Materials, College of Chemistry, Jilin University, Changchun 130012, P. R. China, E-mail: chuandong@jlu.edu.cn

General Information: The UV-Vis-NIR absorption spectra of the solids were recorded by Analytik Jena Specord 210 spectrophotometer with integrating sphere. The fluorescence spectra and absolute fluorescence quantum yield taken at room temperature were carried out on Edinburgh FLS920 steady state fluorimeter. The contact angle is measured by the Contact Angle tester 14004485 DSA-100S. The thermal conductivity of cotton fabric was measured by C-Therm TCi (The probe serial number is H357). Ion concentration after seawater desalination tested by avio 200 inductively coupled plasma emission spectrometer.

Photothermal experiment: Optical and thermal experiments: The morphology of cotton fabric was observed by SEM (EM-30plus). Temperature changes were recorded with an infrared thermal imager (FADER-869). Xenon Cell-S500/350 light source (AM 1.5G spectral filter) was used for water evaporation and thermoelectric power generation. TEC1-12706 is used as thermoelectric device and Keithle 6514 system is used to obtain open circuit voltage data.

Solar steam generation experiments: Solar steam generation experiment: the solar evaporator 3 is fixed with foam at both ends of a plastic container, one end is immersed in water, sunlight is generated by a solar simulator with a standard AM 1.5 G spectrum (CEL-S500/350) filter, and irradiates the evaporator 3 at a specific light concentration. The weight loss of water was measured by an analytical balance, and the temperature of the whole process was recorded by an infrared thermal imager. The energy conversion efficiency was measured.

Solar temperature difference power generation: Commercial thermoelectric generator (TEC1-12706, length 40 mm, width 40 mm, height 3.6 mm) is selected for power generation. Lay the evaporator 3 on the surface of the thermoelectric sheet. The thermoelectric open circuit voltage (VOC) and resistance (Ohm) were measured and recorded using a Keithley 6514 system electrometer. Subsequent power generation

was performed on 1, 2 and 5 kW m^{-2} respectively, and the surface temperature was collected and recorded by an infrared thermal imager.

The thermal conductivity of cotton fabric: The transient plane heat source method selects Pyrex glass as a standard part in the test process, and the reference value of thermal conductivity at 20 ºC is 1.143 W/ (m·K). The thermal conductivity of the material can be obtained by measuring the voltage change of the sensor chip. The thermal conductivity of cotton fabric is 0.048 W/(m·K).

Calculation of the load efficiency of the molecule 3 on the cotton fabric: The load efficiency η of 3 on the cotton fabric was calculated as the following formula:

$$\eta = \frac{m_1 - m_0}{m} = \frac{1.1404 - 1.1385}{0.0020} = 95\%$$

where m_1 is the mass of evaporator 3 (1.1404 g), m_0 is the mass of blank cotton fabric before impregnated (1.1385 g), and m is the mass of molecule 3 powder (0.0020 g). As a result, the load efficiency η = 95%.

Calculation of the efficiency for solar to vapor generation: The conversion efficiency η of solar energy in photothermal assisted water evaporation was calculated as the following formula.

$$\eta = \frac{\dot{m} h_{LV}}{C_{opt} P_0}$$

Where ṁ refers to the mass flux (evaporation rate) of water, h_{LV} refers to the total liquid vapor phase-change enthalpy (i.e., the sensible heat and the enthalpy of vaporization (i.e., $h_{LV} = Q + \Delta h_{vap}$)), Q is the energy provided to heat the system from the initial temperature to a final temperature, Δh_{vap} is the latent heat of vaporization of water P_0 is the nominal solar irradiation value of 1 kW m^{-2}, and C_{opt} represents the optical concentration. The schematic for the vaporization enthalpy of the vapor was as follows.

$$Q = C_{liquid} \times (T - T_0)$$

$$\Delta h_{vap} = Q_1 + \Delta h_{100} + Q_2$$

$$Q_1 = C_{liquid} \times (100 - T)$$

$$Q_2 = C_{vapor} \times (T - 100)$$

In this paper, C_{liquid}, the specific heat capacity of liquid water is a constant of 4.18 (g ^{o}C)$^{-1}$. C_{vapor}, the specific heat capacity of water vaper is a constant of 1.865 J (g ^{o}C)$^{-1}$. Δh_{100} is the latent heat of vaporization of water at 100 ^{o}C, taken to be 2260 kJ kg^{-1}. The surface temperature of the evaporator 3 was 37.7 ^{o}C during the evaporation process, therefore T is 37.7 ^{o}C. As the above fomulas,

$$Q = C_{liquid} \times (T - T_0) = 4.18 \times (37.7 - 24.1) = 56.848\ kJ\ kg\text{-}1$$

$$\Delta h_{vap} = Q_1 + \Delta h_{100} + Q_2 = 4.18 \times (100 - 37.7) + 2260 + 1.865 \times (37.7 - 100)$$

$$= 2404.22\ kJ\ kg\text{-}1$$

$$h_{LV} = Q + \Delta h_{vap} = 56.848 + 2404.22 = 2461.07\ kJ\ kg\text{-}1$$

$$\dot{m} = 1.36\ kg\ m^{-2} h^{-1}$$

$$P_0 = 1000\ W\ m^{-2}$$

$$C_{opt} = 1$$

As a result, evaporation efficiency $\eta = \dot{m} h_{LV} / C_{opt} P_0 = 93\%$ when the latent heat of water vaporization at 37.7 ^{o}C (2461.07 kJ kg^{-1}) is used in calculation.

Supplementary figures and table:

Figure S1. The digital photo of cotton fabric carrier.

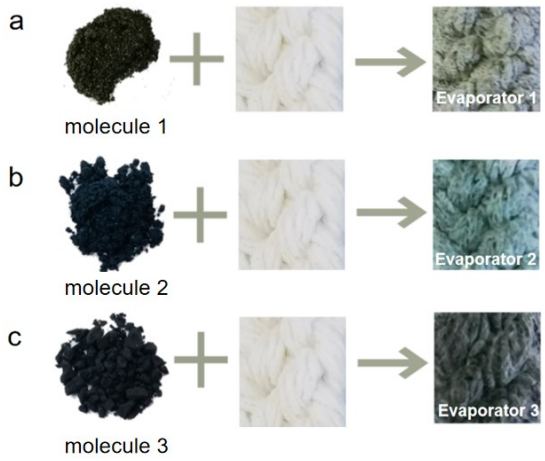

Figure S2. The preparation process of three solar evaporators, a) evaporator 1, b) evaporator 2 and c) evaporator 3.

Figure S3. The loading capacity change of evaporator 3 before and after kneading and folding.

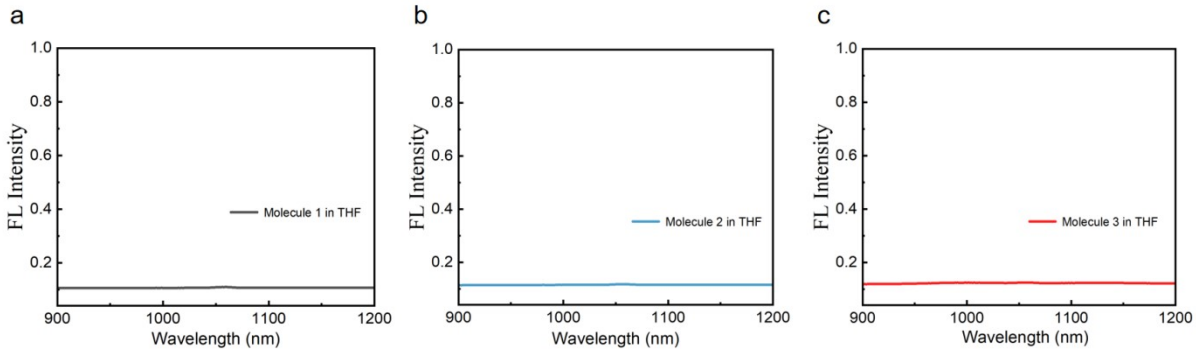

Figure S4. The fluorescence spectra of the molecules in THF solution (20 μg mL^{-1}) excited at 808 nm at room temperature, a) molecule 1, b) molecule 2 and c) molecule 3.

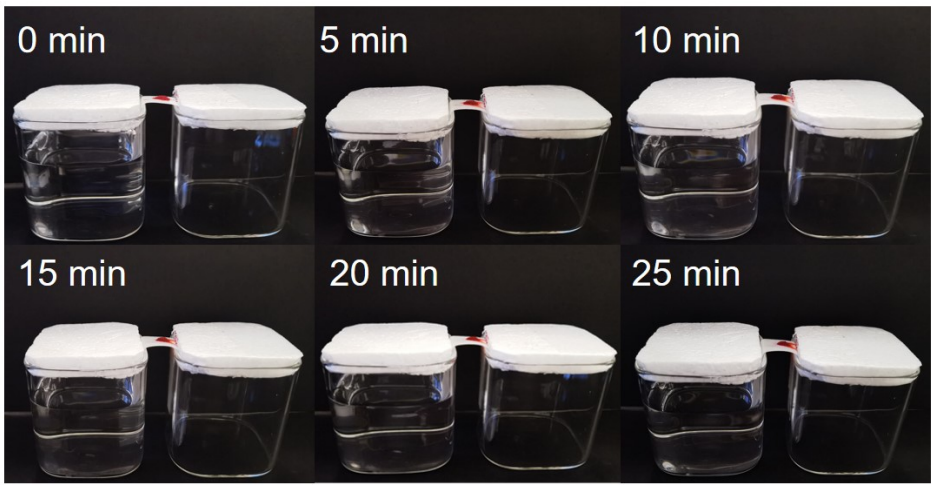

Figures S5. Optical picture time sequences describing the salt removal process of the carrier.

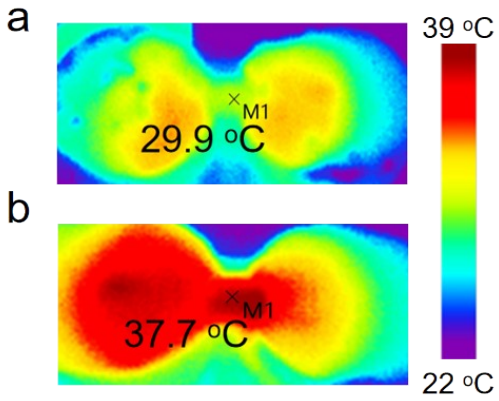

Figure S6. The infrared images of the blank cotton fabric and evaporator 3 in the process of water evaporation: a) blank cotton fabric and b) evaporator 3.

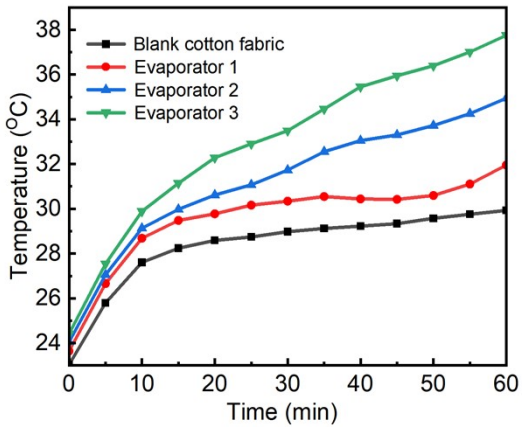

Figure S7. Surface temperature of blank cotton fabric and evaporators during the water evaporation under 1 kW m^{-2} simulated sunlight irradiation.

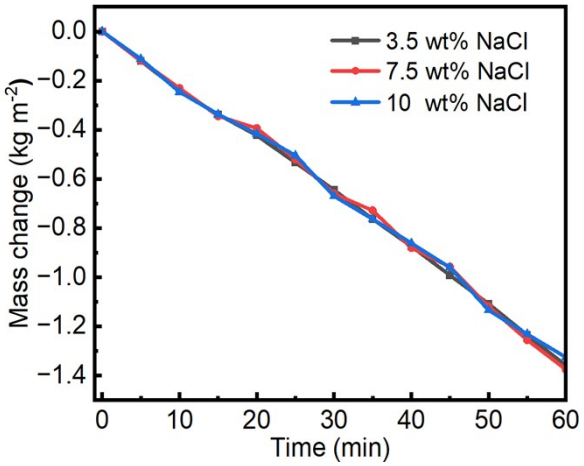

Figure S8. Evaporation rate of evaporator 3 for different salt concentrations under 1 kW m^{-2} simulated sunlight irradiation.

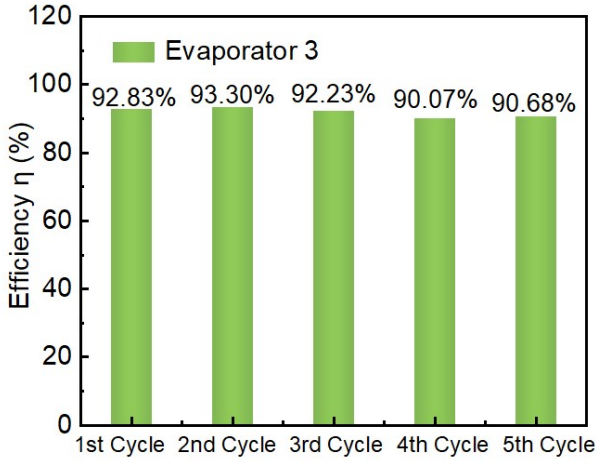

Figure S9. The efficiency of evaporator 3 in 3.5% NaCl solution in five cycles under the irradiation of 1 kW m^{-2}.

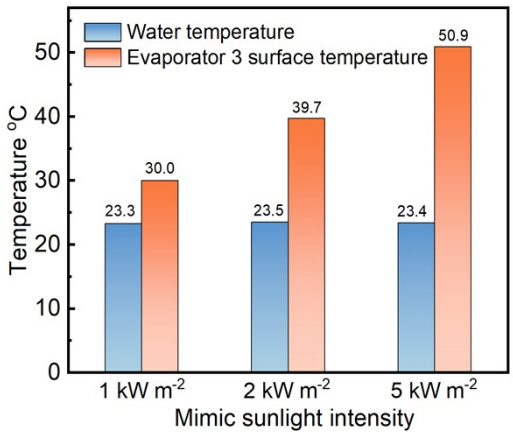

Figure S10. Temperature difference histogram of thermoelectric devices at solar energy densities of 1, 2 and 5 kW m^{-2}.

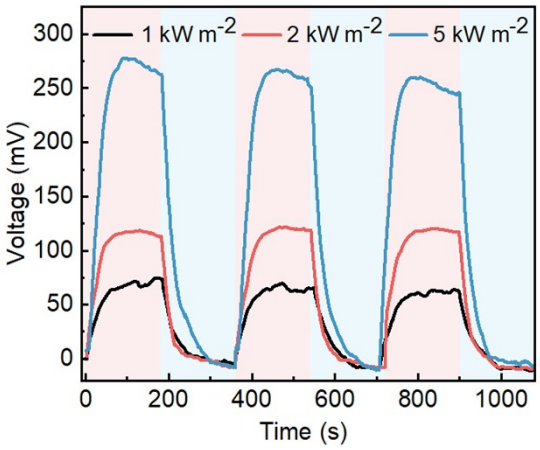

Figure S11. Cycling performance of evaporator 3 under 1, 2, and 5 sunlight.

Table S1. The water evaporation rate and water evaporation conversion efficiency of different photothermal functional materials under 1 kW m^{-2} simulated solar irradiation.

System	Materials	Evaporation rate (kg m^{-2} h^{-1})	Evaporation conversion efficiency (%)	Ref.
Organic small molecule	Molecular 3	1.360	93.00	This work
	DPP	1.304	90.60	1
	DDPA-PDN	1.070	56.23	2
	4OCSPC	1.262	86.60	3

	GDPA-QCN	1.300	90.40	4
	PM6:Y6	1.520	88.90	5
	AFQ	1.330	57.00	6
	TPA-TPA-O_6	1.293	89.41	7
	TPyP	0.810	56.00	8
	CR-TPE-T	1.272	87.20	9
	IDT-O_4	1.365	94.38	10
Organic polymer	CB/MF/EPE	1.240	77.80	11
	PPy@D-SCG	1.540	89.10	12
	GT-COF-3	1.314	90.70	13
	PPy/SS	0.920	58.00	14
	PPy-wood	1.014	72.50	15
	PHT	1.169	80.50	16
	PDA/BNC	1.130	78.00	17
	Nylon-C	1.240	83.10	18
Inorganic	rGO/PU	0.900	65.00	19
	TA/Fe^{3+}-bamnoo	1.152	78.86	20
	HPCM-PHS	1.380	90.80	21
	Mxene/CNTs	1.350	88.20	22
	Carbon fiber	1.300	80.00	23
	Au/D-NPT	0.870	64.00	24
	DLS	1.100	65.00	25
	Ti_3C_2 MXene	1.310	71.00	26
	3D-CG/GN	1.250	85.60	27
	CNT/CNC	1.350	87.40	28

1. X. Zhang, Y. Li, Z. Chen, P. Li, R. Chen and X. Peng, *Dyes Pigments*, 2021, **192**, 109460.

2. Y. Cui, J. Liu, Z. Li, M. Ji, M. Zhao, M. Shen, X. Han, T. Jia, C. Li and Y. Wang, *Adv. Funct. Mater.*, 2021, **31**, 2106247.
3. X. Han, Z. Wang, M. Shen, J. Liu, Y. Lei, Z. Li, T. Jia and Y. Wang, *J. Mater. Chem. A*, 2021, **9**, 24452-24459.
4. J. Liu, Y. Cui, Y. Pan, Z. Chen, T. Jia, C. Li and Y. Wang, *Angew. Chem. Int. Ed.*, 2022, **61**, e202117087.
5. J. Zhu, X. Wang, J. Liang, X. Qiu, S. Chen, Y. Wang and Y. Wang, *EcoMat*, 2023, **5**, e12323.
6. Y.-T. Chen, X. Wen, J. He, Z. Li, S. Zhu, W. Chen, J. Yu, Y. Guo, S. Ni, S. Chen, L. Dang and M.-D. Li, *ACS Appl. Mater. Interfaces*, 2022, **14**, 28781-28791.
7. Z. Wang, J. Zhou, Y. Zhang, W. Zhu and Y. Li, *Angew. Chem. Int. Ed.*, 2022, **61**, e202113653.
8. Y. Zhang, H. Yan, X. Wang, Z. Zhang, F. Liu, S. Tu and X. Chen, *RSC Advances*, 2022, **12**, 28997-29002.
9. G. Chen, J. Sun, Q. Peng, Q. Sun, G. Wang, Y. Cai, X. Gu, Z. Shuai and B. Z. Tang, *Adv. Mater.*, 2020, **32**, 1908537.
10. J. Huang, Z. Wang, W. Zhu and Y. Li, *Aggregate*, 2023, DOI: 10.1002/agt2.426.
11. Y. Xiao, X. Wang, C. Li, H. Peng, T. Zhang and M. Ye, *J Environ Chem Eng*, 2021, **9**, 105010.
12. C. Shi, X. Zhang, A. Nilghaz, Z. Wu, T. Wang, B. Zhu, G. Tang, B. Su and J. Tian, *Chem. Eng. J.*, 2023, **455**, 14036.
13. Y. Y. Li, T. Wei, C. Liu, Z. Zhang, L. F. Wu, M. Ding, S. Yuan, J. Zhu and J. L. Zuo, *Chem-Eur J*, 2023, **29**, e202301048.
14. L. Zhang, B. Tang, J. Wu, R. Li and P. Wang, *Adv. Mater.*, 2015, **27**, 4889-4894.
15. Y. Gu, Z. He, X. Liu, Y. Sun, S. Jiang, H. Liu, G. Liu and J. Luo, *Eur J Wood Prod*, 2023, **81**, 1177-1188.
16. Q. Chen, Z. Pei, Y. Xu, Z. Li, Y. Yang, Y. Wei and Y. Ji, *Chem Sci*, 2018, **9**, 623-628.
17. Q. Jiang, H. Gholami Derami, D. Ghim, S. Cao, Y.-S. Jun and S. Singamaneni, *J. Mater. Chem. A*, 2017, **5**, 18397-18402.
18. Y. Jin, J. Chang, Y. Shi, L. Shi, S. Hong and P. Wang, *J. Mater. Chem. A*, 2018, **6**, 7942-7949.
19. G. Wang, Y. Fu, A. Guo, T. Mei, J. Wang, J. Li and X. Wang, *Chem. Mater.*, 2017, **29**, 5629-5635.
20. P. Zhang, X. Piao, H. Guo, Y. Xiong, Y. Cao, Y. Yan, Z. Wang and C. Jin, *Ind Crop Prod*, 2023, **200**, 116823.
21. X. Ma, W. Fang, Y. Guo, Z. Li, D. Chen, W. Ying, Z. Xu, C. Gao and X. Peng, *Small*, 2019, **15**, 1900354.
22. Y. Wang, Q. Qi, J. Fan, W. Wang and D. Yu, *Sep. Purif. Technol.*, 2021, **254**, 117615.

23. W. Zhao, H. Gong, Y. Song, B. Li, N. Xu, X. Min, G. Liu, B. Zhu, L. Zhou, X. X. Zhang and J. Zhu, *Adv. Funct. Mater.*, 2021, **31**, 2100025.
24. L. Zhou, Y. Tan, D. Ji, B. Zhu, P. Zhang, J. Xu, Q. Gan, Z. Yu, J. Zhu, *Sci. Adv.*. 2016, **2**, e1501227.
25. H. Ghasemi, G. Ni, A. M. Marconnet, J. Loomis, S. Yerci, N. Miljkovic and G. Chen, *Nat. Commun.*, 2014, **5**, 4449.
26. J. Zhao, Y. Yang, C. Yang, Y. Tian, Y. Han, J. Liu, X. Yin and W. Que, *J. Mater. Chem. A*, 2018, **6**, 16196-16204.
27. Y. Li, L. Li, Y. Wu and Y. Li, *The J. Phys. Chem. C*, 2017, **121**, 8579-8588.
28. L. Zhu, T. Ding, M. Gao, C. K. N. Peh and G. W. Ho, *Adv. Energy Mater.*, 2019, **9**, 1900250.